AD_____

Award Number:
W81XWH-08-1-0192

TITLE:
INCORPORATING FUNCTIONAL IMAGING INFORMATION TO rpFNA ANALYSIS FOR BREAST CANCER DETECTION IN HIGH-RISK WOMEN

PRINCIPAL INVESTIGATOR:
Kristy L. Perez

CONTRACTING ORGANIZATION:
Duke University
Durham, NC 27706

REPORT DATE:
March 2010

TYPE OF REPORT:
Annual Summary

PREPARED FOR: U.S. Army Medical Research and Materiel Command
Fort Detrick, Maryland 21702-5012

DISTRIBUTION STATEMENT: (Check one)

X Approved for public release; distribution unlimited

☐ Distribution limited to U.S. Government agencies only; report contains proprietary information

REPORT DOCUMENTATION PAGE

Form Approved
OMB No. 0704-0188

1. REPORT DATE *(DD-MM-YYYY)*	**2. REPORT TYPE**	**3. DATES COVERED** *(From - To)*
31-03-2010	Annual Summary	01 MAR 2009 - 28 FEB 2010

4. TITLE AND SUBTITLE
Incorporating Functional Imaging Information into rpFNA

Analysis for Breast Cancer Detection in High-Risk Women

5a. CONTRACT NUMBER

5b. GRANT NUMBER
W81XWH-08-1-0192

5c. PROGRAM ELEMENT NUMBER

6. AUTHOR(S)
Kristy Perez
Email: kristy.perez@duke.edu

5d. PROJECT NUMBER

5e. TASK NUMBER

5f. WORK UNIT NUMBER

7. PERFORMING ORGANIZATION NAME(S) AND ADDRESS(ES)

Duke University
Office of Sponsored Programs
Box 104135
Durham, NC 27708
E-mail: klp14@duke.edu

8. PERFORMING ORGANIZATION REPORT NUMBER

9. SPONSORING / MONITORING AGENCY NAME(S) AND ADDRESS(ES)
US Army Medical Research and Material Command
Fort Detrick, MD 21702-5012

10. SPONSOR/MONITOR'S ACRONYM(S)

11. SPONSOR/MONITOR'S REPORT NUMBER(S)

12. DISTRIBUTION / AVAILABILITY STATEMENT
Approved for public release; distribution unlimited

13. SUPPLEMENTARY NOTES

14. ABSTRACT
The overall goal of this work is to correlate the imaging information from the dual-modality, dedicated single photon emission computed tomography (SPECT) and computed tomography device with the results of random periareolar fine needle aspiration (rpFNA) in women at high risk for breast cancer. In this second year of work, efforts have been concentrated on quantifying the SPECT image signal by correctly modeling the physics in the reconstruction code including attenuation and scatter. Experiments were completed to show the quantification algorithm produces linear results from 0.03 uCi/mL to 30 uCi/mL. Additionally, further investigation into the potential of imaging the radioactive rpFNA needles with our current semiconductor camera revealed that it was not likely the needles would contain enough radioactivity to be distinguished above background. Work resulting from this project was presented at a local seminar and international conference this year and several manuscripts are being submitted for peer review.

15. SUBJECT TERMS
Nuclear Medicine Imaging, SPECT, Molecular Breast Imaging, Mammotomography, rpFNA

16. SECURITY CLASSIFICATION OF:			**17. LIMITATION OF ABSTRACT**	**18. NUMBER OF PAGES**	**19a. NAME OF RESPONSIBLE PERSON**
a. REPORT	**b. ABSTRACT**	**c. THIS PAGE**			Kristy Perez
Unclassified	Unclassified	Unclassified	Unlimited	20	**19b. TELEPHONE NUMBER** *(include area code)* 919-684-7943

Table of Contents

A. Introduction

The overall goal of this work is to correlate the imaging information from our dual-modality, dedicated single photon emission computed tomography (SPECT) and computed tomography (CT) device with results of random periareolar fine needle aspiration (rpFNA) in women at high risk for breast cancer. The quantitative functional imaging signal from the whole breast will be compared to the histological rpFNA analysis. In this second year of work, appropriate corrections to the image formation process have been made such that the reconstructed SPECT images are quantitative and are displayed in units of μCi/mL. I have additionally fulfilled other aspects of the training program, including attending local and international conferences and drafting papers for peer review.

B. Body

The Statement of Work and proposed timeline are included in Appendix A. For Year 2, the tasks outlined preparations for and initiation of collecting and correlating patient SPECT-CT and rpFNA data. SPECT signal quantification has been investigated and is achievable to better than 15% accuracy.

Task 1: Acquire IRB approval

Task 1(a): Participate on writing IRB protocol for FMT imaging in a high risk patient cohort.

The institutional review board (IRB) protocol for this study has been drafted and will be submitted shortly. Note that the primary grant supporting that submission is my advisor's NIH funded grant (R01-CA096821) which includes imaging women with known or suspected breast cancer. After completing tasks 3(a)-(b), we have decided to further stratify the rpFNA patient cohort to include the patients which we think would potentially benefit the most while giving information about the image signal at various stages of breast cancer development – specifically imaging women at high risk for both breast cancer and heart disease. Because ^{99m}Tc sestamibi was originally developed for cardiac imaging, we think that a cohort of women who could benefit from both breast and cardiac imaging would be able to also provide us with information about the metabolic activity of the whole breast and of various morphologies of breast tissues (normal, atypical, malignant, etc).

Task 2: Evaluate radioactive needles for guided histology

In the last reporting period it was decided to use GEANT4, a Monte Carlo physics simulation package, to model the radioactive needles and imaging system to determine the appropriate approach to image/measure the activity and distribution in the needles. In continuing that line of research, new information about the quantity of activity in the breast was found. The median, 10th percentile and 90th percentile uptake of asymptomatic/normal breast tissue has been measured to be 0.047 μCi/mL, 0.032 μCi/mL and 0.072 μCi/mL, respectively [1]. Therefore, it is calculated that in the 1.5 inch, 21-gauge aspiration needle (volume = 0.0079 mL) there will be a total of 0.00055 μCi or 20.5 decays/sec. For our system, it is exceptionally unlikely we will be able to image/measure the needle signal above the background (~1 count/sec) because the gamma camera has pixilated detector elements (each 0.25x0.25 cm^2 over a large overall area of 16x20 cm^2) and has a sensitivity considerably less than 0.50%. An alternative option for quantifying the activity in the needle is a considerably higher detection efficiency well counter, but no spatial information along the length of the needle would be available, and the length of time to measure the needle make it clinically impractical. Therefore, we are not currently intending to go forward with this specific aim, but rather focus efforts on relating image quantification with histology results.

Task 3: Optimize patient imaging and biopsy protocol.

Task 3(a): Investigate how the dedicated SPECT imaging and biopsy procedures can be optimally integrated to minimize the patient scan times.

Because we have decided not to pursue imaging the rpFNA needles, volunteers do not necessarily need to have the SPECT-CT imaging and rpFNA on the same day or at the same location. Volunteers can be imaged one day in our laboratory and the next day (or any time after SPECT imaging) have the rpFNA procedure completed in its normal location.

To confirm normal tissue radioactivity uptake quantities found in literature, we are proposing to image patients who are being imaged for heart disease. ^{99m}Tc sestamibi, originally developed for cardiac imaging, is used in rest-stress studies of the heart to diagnose cardiac abnormalities. Because these women will already be injected with the radiation, the only additional inconvenience to the patient is an hour of her time for the additional imaging. Note that there will be no additional injection of radioactivity or exposure of the patient to any risks for the proposed additional imaging.

Task 3(b): Investigate how the information gained with SPECT imaging can be incorporated into the biopsy procedure.

Radiotracer uptake in focal lesions and the entire breast volume directly relates to the mitochondrial activity of the cells therein [2]. Comparing this mitochondrial signal with the mitochondrial disregulation studied as part of the rpFNA procedure for a variety of cellular morphologies may provide insight into the types of atypia and ductal carcinoma in situ (DCIS) which eventually leads to invasive disease. However, accurate absolute activity quantification is of paramount importance to make comparisons of relatively small radioactivity concentrations. Physical processes and, with systems capable of 3D trajectories, reconstruction artifacts can yield an incorrect absolute activity of the tracer. Over the course of this reporting period, an algorithm (Figure 1) to quantify the SPECT signal was developed and tested.

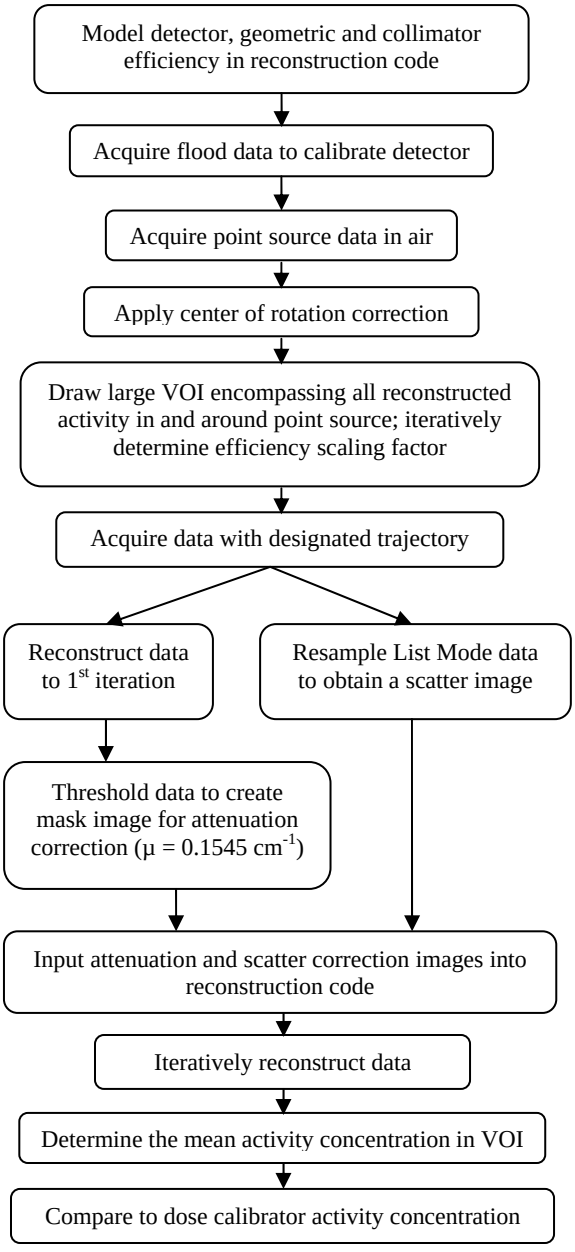

FIGURE 1: Flowchart depicting necessary steps for quantifying SPECT data.

Differences in the obtained activity value from three trajectories – vertical axis of rotation (VAOR), 30° tilted parallel beam (TPB), and projected sinusoidal wave (PROJSINE) – were investigated to determine if the acquisition trajectory can be used for quantification. For these experiments, fillable geometric and anthropomorphic phantoms containing aqueous ^{99m}Tc pertechnetate were imaged with the dedicated dual-modality SPECT-CT scanner. SPECT images were collected with 128 projections of each trajectory. Collimator and detection efficiencies of the SPECT camera were incorporated into the OSEM iterative reconstruction. Attenuation correction was implemented using a uniform attenuation coefficient matrix, but in subsequent trials will be done with scaled volumetric CT images obtained from our system (see Madhav W81XWH-06-1-0791, final report). In addition, a Compton Window scatter correction method was applied with an empirically determined k value and a scatter window abutting and below the primary photopeak window. Three different photopeak windows and consequently scatter windows (Table 1) were investigated to

determine if the inclusion/exclusion of some primary counts and partial charge collection counts due to the CZT detector would affect the accuracy, SNR and contrast of the known hot spots.

Table 1: Scatter energy windows and scatter fractions for each photopeak energy window

Photopeak Window Width (%)	**Scatter Peak** (keV)	**Energy Range** (keV)	**Scatter Fraction** (k value)
±4	123	113 – 133	0.16
±8	109	92 – 127	0.26
-16+8	94	71 – 116	0.92

Three 30mL syringes filled with 10mL of varying concentrations of radioactivity (Table 2) in a cylindrical phantom were quantified as previously mentioned to determine the linearity and accuracy of the quantification technique, and the SNR and contrasts were also compared for each energy window and trajectory (Figures 2-4).

Table 2: Initial radioactivity and activity concentration in syringes and cylinder

	Activity (uCi)	**Volume** (mL)	**Activity Conc** (uCi/mL)
Syringe 1	34.7	9.7	3.6
Syringe 2	113.3	10	11.3
Syringe 3	226.8	11	20.6
Background	386.8	900	0.430

The decay corrected, mean activity concentration has good agreement with “known” values determined from dose calibrator measurements, which were considered as the gold standard (Figure 2). The results indicate that the accuracy has some dependence on the presence of a scatter/attenuating medium, source activity concentration, energy window and acquisition trajectory. For lower activity concentrations, the accuracy is worse than for greater amounts of activity (Figure 3). Note that the greatest difference is in images with air background, potentially due to the scatter factor over compensating when no background medium is present. Generally, the accuracy is better than 15% for activity concentrations >3μCi/mL. The 24% energy window data is the least accurate and 8% and 16% data are very similar (Figure 3). For the data with water plus radioactive background, the variability between scans is generally less than 10% for all three acquisition trajectories.

SNR and contrast of each syringe in a radioactive background for the different energy windows are displayed in Figure 4. The -16/+8% energy window generally has the smallest contrast with no gains in SNR compared to the other energy windows. The results indicate that the ±8% would provide the same quantitation as the ±4% but with gains in SNR. The SNR for the VAOR trajectory is better than for the TPB or PROJSINE, while the contrast is about the same.

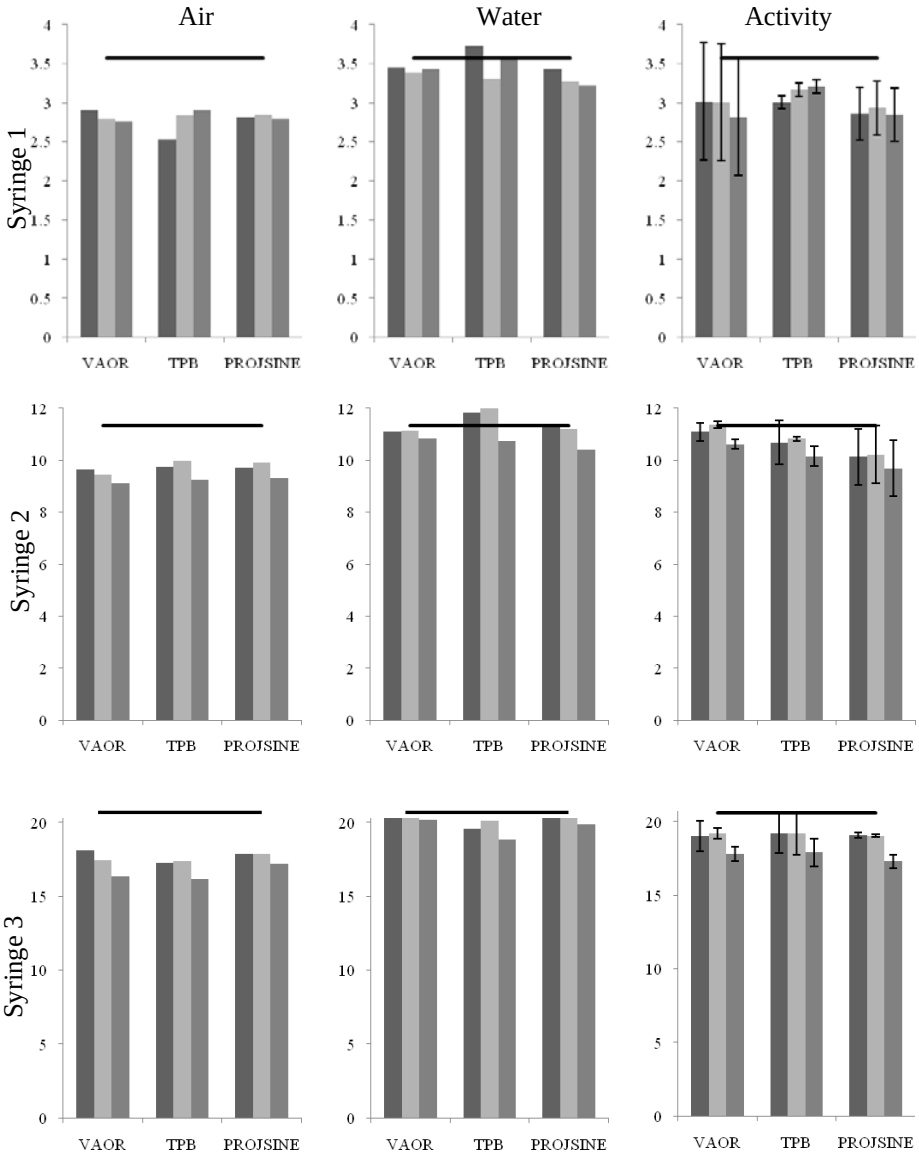

FIGURE 2: Bar charts of dose calibrator (black lines) and decay corrected image measured activity concentrations for 8% (dark grey), 16% (light grey) and 24% (medium grey) energy windows for syringes 1 (TOP), 2 (MIDDLE), and 3 (BOTTOM) and for air (LEFT), water only (CENTER), and aqueous radioactive (RIGHT) backgrounds. Error bars for two sequential scans when radioactive background is present are shown (right).

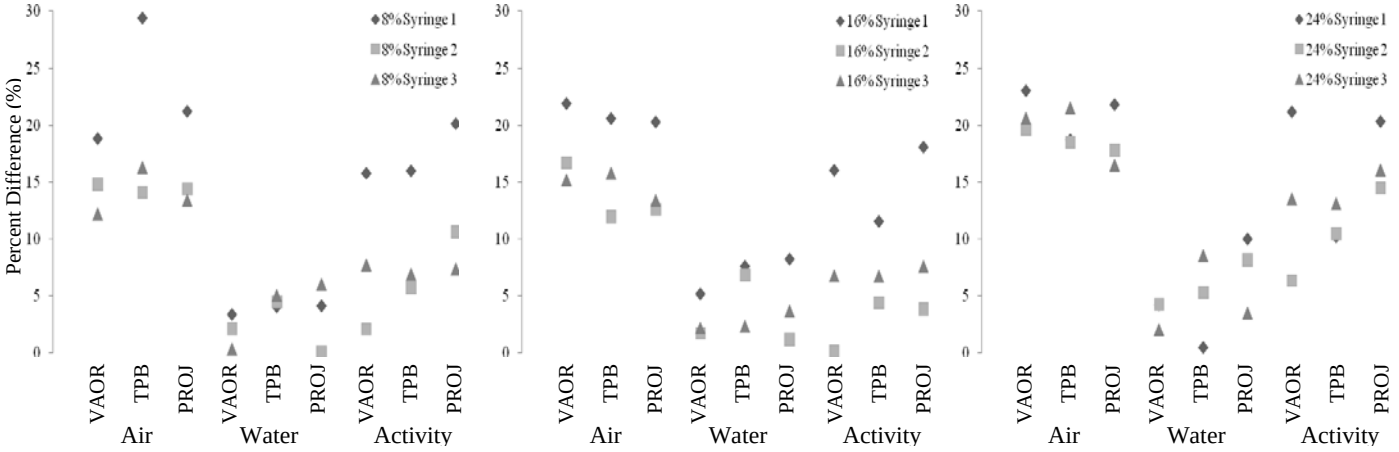

FIGURE 3. VAOR, TPB and PROJSINE percent difference for each background compared the dose calibrator value. 8% (LEFT), 16% (CENTER) and 24% (RIGHT) energy windows for each syringe and trajectory. Note that the greatest difference is in images with air background, potentially due to the scatter factor over compensating when no background medium is present.

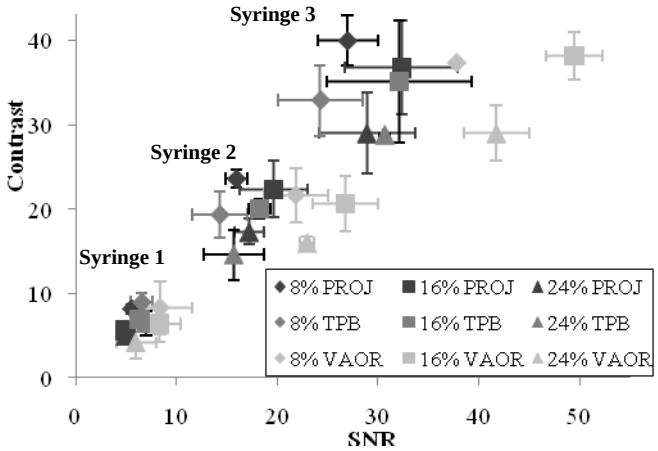

FIGURE 4. SNR versus contrast from second iteration coronal reconstructed images for syringes 1, 2, and 3 in a radioactive background for different acquisition orbits and energy windows. Error bars represent the standard deviation from the two sequential scans.

Additionally, an 800 mL anthropomorphic breast phantom was imaged, containing a 2.3 mL acrylic-walled sphere (*Radiological Service Devices Inc.*, Newport Beach, CA) and a 1.6 mL thin-walled balloon (*Harvard Apparatus*, Holliston, MA) filled with aqueous ^{99m}Tc pertechnetate. Table 3 gives the initial radioactive concentrations, measured with a dose calibrator, of the spheres and background.

Table 3: Initial radioactivity and activity concentration of the spheres and breast phantoms

	Activity (uCi)	**Volume** (mL)	**Activity Conc** (uCi/mL)
Acrylic	28.4	2.3	12.3
Balloon	19.8	1.6	12.4
Background	222.6	765	0.291

Corrected, reconstructed and analyzed as before, the accuracy, SNR and contrast were compared. VAOR and PROJSINE spherical lesion data are accurate to within 15%, while TPB data have consistently greater than 30% deviation from the actual dose calibrator measured concentration (Figure 5). Because the TPB data is insufficiently sampled, elongation artifacts in the reconstructed images distort the shape of the breast and lesions, dispersing the activity into a greater image volume. Additionally, there is an attenuation map inconsistency given the elongation artifact, and the known, smoothly varying, true phantom distribution. Therefore, the total activity is dipersed over the larger volume, and consequently the activity concentration reported in each voxel decreases.

Figure 6 shows a plot of the average SNR and contrast of the two lesions from two sequential scans of each trajectory and energy window. The TPB trajectory produced images with the best SNR and contrast, probably because the gamma camera is able to image relatively closer to the lesions than the other trajectories. Comparing just the VAOR and PROJSINE trajectory, VAOR has a higher SNR and PROJSINE has a higher contrast, for the respective energy windows. The 24% energy window had the best SNR and equivocal contrast performance for the acrylic lesion, while it is difficult to say which energy window had the best SNR or contrast performance for the balloon lesion.

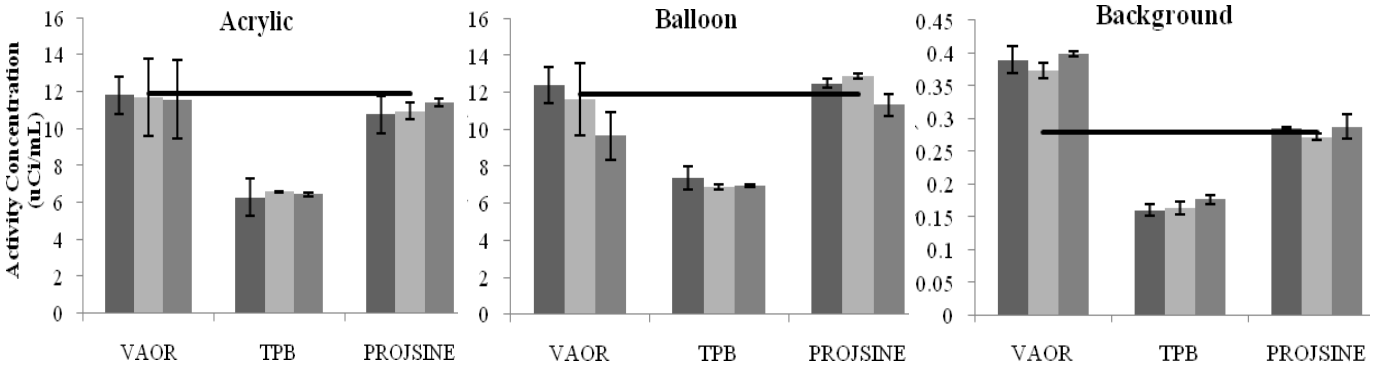

FIGURE 5. Bar charts of dose calibrator (black lines) and corrected image measured activity concentration for the acrylic (LEFT) and balloon lesions (MIDDLE) and uniform breast background (RIGHT) for the 8% (dark gray), 16% (light gray) and 24% (medium gray) energy windows.

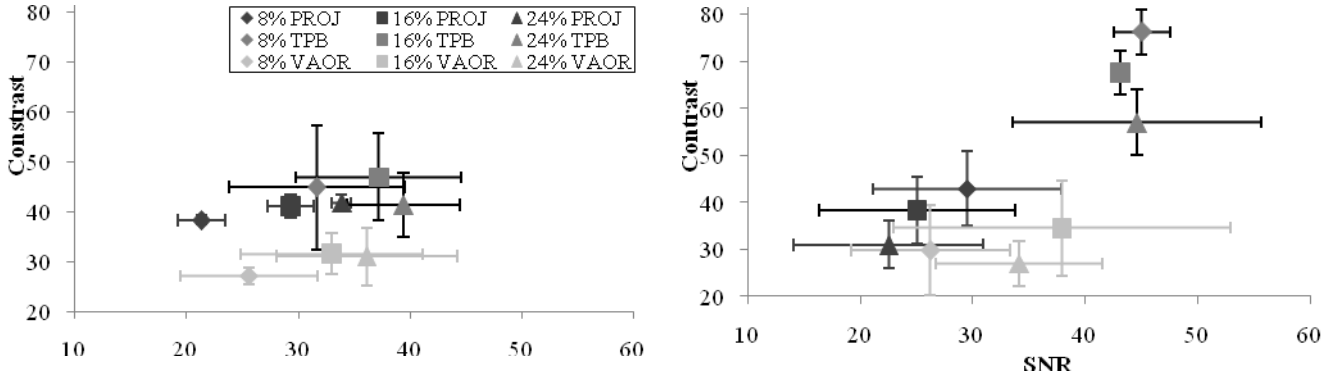

FIGURE 6. SNR and contrast of acrylic (LEFT) and balloon (RIGHT) lesions. Error bars represent the standard deviation from the two sequential scans.

Upon learning normal breast tissue uptake is likely between 0.032 and 0.072 μCi/mL [1], further tests of the linearity of the system over a smaller activity concentration range were undertaken. For this study, various breast phantoms were filled with 470, 935 and 1060mL aqueous ^{99m}Tc-pertechnetate and imaged with our CZT-based breast SPECT system with a ±4% energy window. The initial breast activity concentration was ~0.3 μCi/mL and planar and SPECT-CT images were acquired at 3 hr time intervals until decaying to ~0.03 μCi/mL. Heart, liver and partial torso phantoms were filled at proportional clinical concentration ratios to simulate posterior background activity. Mean values from whole breast volumes of interest generated from fused data were compared with dose calibrator measured values. Three sequential scans were acquired with a PROJSINE acquisition trajectory to evaluate image variability at different activity concentrations. Compared with the time-decayed dose calibrator measured value, the measured data have mean squared errors of 0.004, 0.007 and 0.003 for the 470, 935 and 1060mL breasts, respectively. Plotted against the known activity concentrations, the measured activity concentration R^2 values for linear fits are 0.986, 0.967 and 0.997 with slopes of 1.00, 1.09 and 0.87 for each breast, respectively.

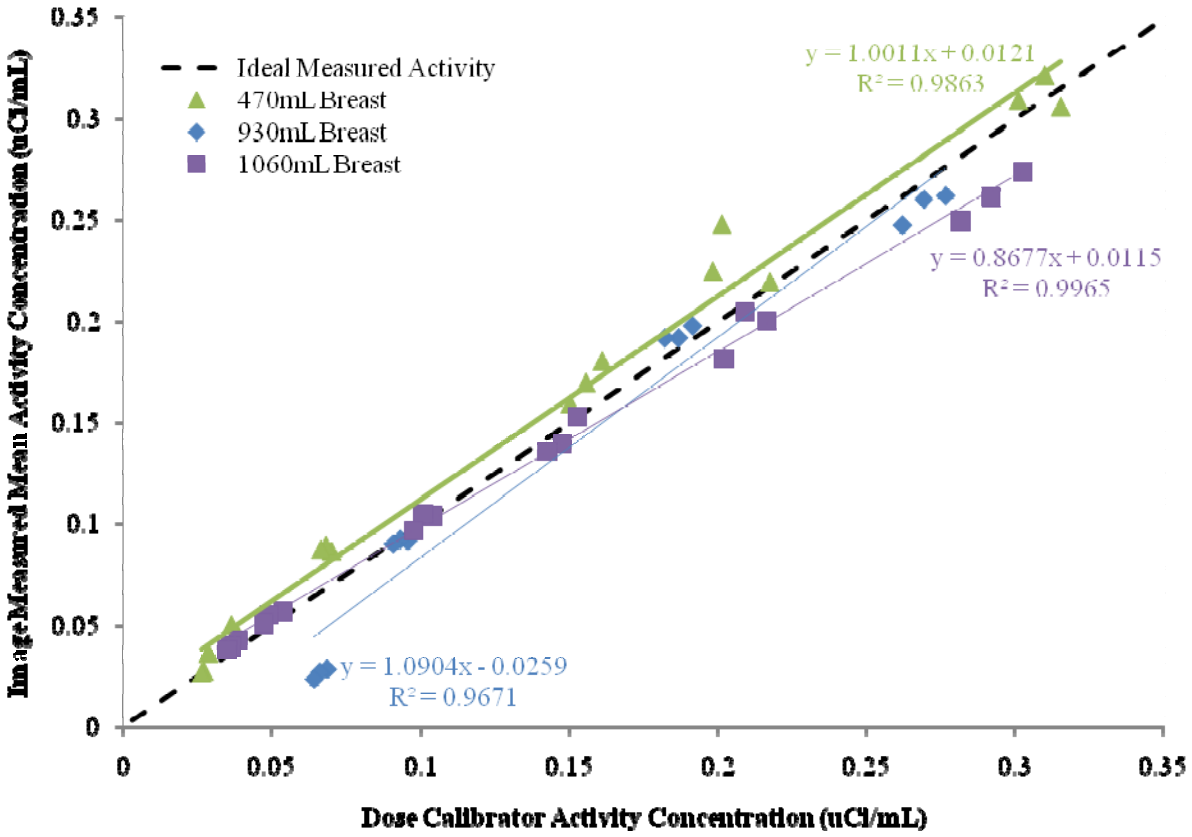

FIGURE 7: Plot of the mean measured activity concentration as a function of the dose calibrator activity concentration. Three acquisitions for each activity concentration were obtained to examine the variability in the image acquisition and quantification method. The accuracy of the method does not seem to be dependent on the activity concentration over the tested range.

A method to quantify the activity concentration of regions and volumes of interest in data acquired with our unique dedicated breast SPECT system has been implemented. The average activity concentration reported in hot-volume regions corresponds to within 15% of the actual measured activity concentrations. Larger errors occur in diffuse background regions of VAOR and TPB images. The cause of which is unknown. However, when this procedure was used to quantify lower activity concentrations with the PROJSINE trajectory the results were once again very close to the known value, indicating the robustness of the method. Therefore, the approach can reasonably accurately quantify low level whole breast activity concentrations in a variety of breast shapes and sizes, giving this approach the potential for discerning minute changes in broad-breast tracer uptake.

For focal hot-spots in anthropomorphic breast phantoms, VAOR and PROJSINE data have better than 15% accuracy with respect to the absolute activity concentration. Insufficiently sampled TPB data, not unexpectedly, has the worst accuracy but otherwise has the redeeming quality of having high quality images. The validity of these results should be retested at lower activity concentrations to determine the accuracy of VAOR and PROJSINE trajectories.

Comparing ±4%, ±8% and -16+8% photopeak energy windows, the accuracy of quantifying low activity concentration regions by utilizing more of the photopeak events (increasing the counting statistics) was investigated. The largest energy window in most cases produced the least accurate quantification. This result could be due to the scatter correction method used where counts were subtracted in proportion to a lower scatter energy window. For this very large energy window, the scatter proportionality constant was large, thus potentially subtracting the benefits of the large window. The 24% wide energy window also produced the images with the lowest contrast, indicating this energy window should not be selected for either quantitative or qualitative imaging. In most cases, the 16% energy window had better accuracy and SNR with little difference in contrast than the 8% energy window.

Additional future steps to improve results would include using the CT reconstructed data set to define the ROI for better placement. To analyze the mean activity concentration in the syringes, relatively large ROIs

placed well within the boundaries of the syringe were used, minimizing partial volume effects. However, for smaller and/or irregularly shaped hot spots (lesions), ROI placement has a large effect on the measured mean activity concentration. Thus, having a CT selected ROI would give more confidence in the measurement.

Task 3(c): Image Patients.

The quantification procedure was retrospectively applied to a 54 year old women with biopsy confirmed ductal carcinoma in situ (DCIS) near her chest wall (Figure 8). The mean value of a volume of interest defined by the CT (Figure 8, gray scale) has a value of 0.04 μCi/mL. This value is within the "normal tissue" range, despite that the image shows evidence of focal hot-spots of DCIS. Nonetheless, these results are promising because 1) we have quantified patient data within the activity concentration range found in literature, and 2) it appears, we can image uptake of the sestamibi tracer in DCIS.

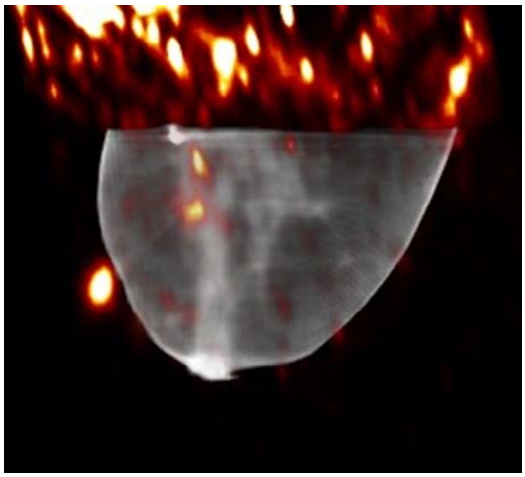

FIGURE 8: Fused SPECT-CT image. SPECT image is displayed in the "hot" scale, (red, orange and yellow) while the CT image is displayed in the gray scale. The CT boundary is used to delineate the volume of interest for SPECT quantification. The average activity value in the SPECT image is 0.04 μCi/mL, within the documented normal range (0.03-0.07 μCi/mL).

Task 4: Complete other aspects of breast cancer training program

Task 4(b): Publish research work in peer-reviewed journals

In November, I submitted a manuscript to *Physics in Medicine and Biology* entitled "Characterizing the contribution of cardiac and hepatic uptake in dedicated breast SPECT using tilted trajectories". Additionally, two manuscripts, currently being reviewed by co-authors, are nearly ready to be submitted to *IEEE Transactions on Nuclear Science*.

Task 4(c): Attend and present at local seminars and conferences

I have attended and presented at several local conferences and seminars, including but not limited to Duke SPORE Breast Cancer meetings, Duke Comprehensive Cancer Center Annual Meeting, Medical Physics Journal Club, national IEEE meeting, and the medical physics weekly seminar.

Task 4(d): Attend international conferences

I attended and gave a poster presentation at the *IEEE Nuclear Science Symposium and Medical Imaging Conference* in Orlando, FL in October 2009. The presentation was well received at the conference, and I

obtained useful feedback and suggestions on this work. I have also been accepted to present a poster at the upcoming 2010 *Society of Nuclear Medicine Annual Meeting* in Salt Lake City, Utah.

C. Key Research Accomplishments

Continuing progress on tasks 2-4 was to be made in Year 2. Task 2 was investigated, and based on the negative results we concluded that information from the radioactive rpFNA needles may not be as valuable as previously thought due to the very low volume and activity contained in each, as well as the rpFNA bulk processing methods. Tasks 1 and 3(a)-(b) have been initiated, and research continues at this time. Progress has been made for each task as follows:

- An IRB protocol has been drafted and is awaiting submission.
- Information about the radioactive uptake of normal tissue coupled with the dimensions of the rpFNA needle indicates it is not likely that imaging the needles after aspiration will result in a distinct signal above system noise. Furthermore, the usefulness of quantity and distribution of activity along the length of the needle with the current method of rpFNA is questionable.
- Refined and tested the procedure to quantify the activity measured in SPECT images.
- Discussed plan for selecting rpFNA patients to image. Patients who are also at high risk for heart disease may be an advantageous sub-group to image because they could potentially have both breast and cardiac imaging acquired with one radioactive injection.

D. Reportable Outcomes

Conference Proceedings

KL Perez, SJ Cutler, P Madhav, MP Tornai. "Towards Quantification of Dedicated Breast SPECT Using Non Traditional Acquisition Trajectories." Presented at the *2009 IEEE Medical Imaging Conference* and published in *IEEE Conference Record NSS/MIC*, Orlando, FL, USA 25-31 Oct 2009.

Accepted for Publication

SJ Cutler, **KL Perez**, HX Barnhart, MP Tornai. "Observer Detection Limits for a Dedicated Breast SPECT Imaging System." Accepted for publication in *Physics in Medicine and Biology*.

In Preparation for Publication

KL Perez, SJ Cutler, P Madhav, MP Tornai. "Characterizing the Contribution of Cardiac and Hepatic Uptake in Dedicated Breast SPECT using Tilted Trajectories." Submitted to *Physics in Medicine and Biology*.

SJ Cutler, **KL Perez**, P Madhav, MP Tornai. "Comparison of 2D Scintimammography and 3D Dedicated Breast SPECT Using A Compressible Breast Phantom and Lesions of Varying Size and Tracer Uptake." In preparation for submission to *Nuclear Medicine Communications*.

KL Perez, SJ Cutler, P Madhav, MP Tornai. "Towards Quantification of Function Breast Images using Dedicated SPECT with Non-Traditional Acquisition Trajectories." Preparing for submission to *IEEE Transactions on Nuclear Science*.

KL Perez, SJ Cutler, MP Tornai. "Empirical Effects of Angular Sampling and Background Content on Image Quality in Dedicated Breast SPECT." Preparing for submission to *IEEE Transactions on Nuclear Science*.

E. Conclusions

In Year 2, progress was made for Task 1, Task 2 and Tasks 3(a)-(b). A working procedure for quantifying radioactive uptake in the breast has been tested and verified. This quantitative information will be used to compare with the probability score reported in rpFNA. Additionally comparing the mitochondrial activity reported by the radioactive tracer with the rpFNA analysis will be investigated. A major effort in Year 2 has produced several manuscripts nearing publication.

F. References

[1] M. O'Connor, S. Phillips, C Hruska, D. Rhodes and D. Collins, "Molecular Breast Imaging: Advantages and Limitations of a Scintimammographic Technique in Patients with Small Breast Tumors," *Breast J.* vol. 13, no.1, pp. 3-11, 2007.

[2] L. Delmon-Moingeon, D. Piwnica-Worms, A. Van den Abbeele, B. Holman, A. Davison, and A. Jones, "Uptake of the Cation Hexakis(2-methoxyisobutylisonitrile)-Technetium-99m by Human Carcinoma Cell Lines *in Vitro*," *Cancer Research*, vol. 50, pp. 2198-2202, 1990.

APPENDIX A: STATEMENT OF WORK

Task 1 Acquire IRB approval to conduct SPECT patient studies and image planar needles (Months 1-6)

a. Participate on writing IRB protocol for FMT imaging in a high risk patient cohort. (Month 1)
b. Modify rpFNA IRB protocol (PI: Seewaldt #4245) to include imaging of planar needles extracted from patient breasts. (Month 1)

Task 2 Evaluate radioactive needles for guided histology (Months 1-36)

a. Design shielded holder or sleeves to image the individual signal from each biopsy needle. (Months 1-3)
b. Construct holder. (Month 4)
c. Use phantoms to test designed holder, and modify as necessary. (Month 5)
d. Obtain 2D image of biopsy needles. (Month 6-36)
e. Analyze the 2D images to determine which needles should be histologically evaluated. (Months 6-36)
f. Determine if there is a statistical correlation between the histology results and the 2D molecular images. (Months 6-36)

Task 3 Optimize patient imaging and biopsy protocol (Months 1-36)

a. Investigate how the dedicated SPECT imaging and biopsy procedures can be optimally integrated to minimize the patient scan times. (Month 1-3)
b. Investigate how the information gained with SPECT imaging can be incorporated into the biopsy procedure. (Months 1-3)
c. Image patients. (Months 6-36)
d. Analyze SPECT studies of returning patients to determine variability in patient setup and image acquisitions. (Months 12-36)

Task 4 Complete other aspects of breast cancer training program (Months 1-36)

a. Shadow a radiologist(s) to observe clinical and diagnostic side in breast cancer imaging (Nuclear Medicine, Mammography). (Months 1-12)
b. Publish research work in peer-reviewed journals. (Months 1-36)
c. Attend and present at local seminars offered at Duke University through Medical Physics and the Breast and Ovarian Oncology Research Program, which is part of the Duke Comprehensive Cancer Center. (Months 1-36)
d. Attend international conferences such as DOD BCRP Era of Hope Meeting, IEEE Medical Imaging Conference, RSNA Conference, Society of Nuclear Medicine or San Antonio Breast Cancer Symposium. (Months 1-36)
e. Prepare and defend thesis. (Months 30-36)

APPENDIX B: CONFERENCE PROCEEDING

Towards Quantification of Dedicated Breast SPECT Using Non-Traditional Acquisition Trajectories

Kristy L. Perez *IEEE Student Member*, Spencer J. Cutler *IEEE Student Member*, Priti Madhav *IEEE Student Member*, Martin P. Tornai *IEEE Senior Member*

***Abstract*- Quantification of radiotracer uptake in lesions can provide valuable information to physicians in deciding patient care or determining treatment efficacy. Physical processes (e.g. scatter, attenuation), detector/collimator characteristics, sampling and acquisition trajectories, and reconstruction artifacts contribute to an incorrect absolute measurement of tracer activity and distribution. For these experiments, a cylinder with three syringes of varying radioactivity concentration, and a fillable 800mL breast with two lesion phantoms containing aqueous ^{99m}Tc pertechnetate were imaged using the SPECT sub-system of the dual-modality SPECT-CT dedicated breast scanner. SPECT images were collected using a compact CZT camera with various 3D acquisitions including vertical axis of rotation, 30° tilted, and complex sinusoidal trajectories. Quantitative differences in the measured absolute activity values were investigated for each acquisition trajectory to determine the efficacy of an acquisition trajectory to quantify regions of focal uptake. With attenuation and scatter corrections applied, reconstruction image results showed that the measured average activity concentrations in the hot-spot areas corresponded to within 15% of the actual dose calibrator measured activity concentration. More complete sampling trajectories outperform incomplete tilted acquisition trajectories.**

I. Introduction

Quantification is not common for routine SPECT imaging. Generally, nuclear medicine physicians rely on differences in relative radioactive tracer uptake patterns to analyze molecular SPECT images. Quantification of the radioactive uptake in the images requires careful application of data corrections. Because radiotracers can be designed to label metabolic processes, receptors, and the like, their absolute *in vivo* quantification of concentration could be a valuable diagnostic tool to differentiate between benign and malignant tissue. Particularly in breast cancer patients, distinguishing absolute *in vivo* quantification via non-invasive molecular imaging could affect a patient's treatment plan.

There are a variety of physical factors that can affect the quantification in SPECT images [1]. These include photon attenuation and scatter which have both been shown to degrade images and hence, various methods have been proposed to correct for these. Attenuation correction relies on obtaining a spatial distribution of attenuation coefficients to model the imaged object, often derived from computed tomography (CT) data, and compensates for non-uniform attenuation. There have been many scatter correction techniques derived over time. For ^{99m}Tc imaging, the Jazsczak or Compton Window Method uses an energy window abutting the photopeak, but lower in energy, to estimate the scatter fraction in the photopeak [2].

Additionally, corrections for system factors, such as the detector, collimator and geometric efficiencies, must be incorporated. These efficiencies scale detected and recorded events to the actual volumetric activity at the time of imaging.

Other groups have investigated quantitative breast imaging using planar single photon imaging techniques [4,5] and have shown that quantification of size and uptake has implications for staging disease [4]. In spite of this, due to the nature of planar imaging, it becomes difficult to correctly quantify smaller volumes. SPECT can localize the disease in 3D space and quantify its absolute radiotracer uptake without added activity from "normal" background tissue [1]. Because our dedicated SPECT system has a fully 3D range of motion, we are able to sample into the chest wall and axilla of the breast [6].

In this study, quantification is implemented on our dedicated SPECT to test the system's linearity in measuring radiotracer uptake. In particular, the effect of data acquired with non-traditional, non-circular trajectories on absolute quantification of SPECT data is observed.

II. Methods

A. Gamma Camera and Data Acquisition

The SPECT sub-system of the hybrid imaging device consists of a Cadmium-Zinc-Telluride (CZT) *LumaGEM* 3200S™ gamma camera (*Gamma Medica Inc.*, Northridge, CA) that has 2.3x2.3 mm crystals with a 6.7% intrinsic FWHM at 140 keV and a sensitivity of 37.9 cps/MBq (Fig. 1). The lead parallel hole collimator has 1.22 mm flat-to-flat hexagonal holes with 0.2 mm septa and is 25.4 mm in height. The camera system is attached to precision positioning motors to permit movement in 3D to contour the breast surface by moving in and out, up and down and around the center of rotation. Previous work has defined a set of trajectories which maximize the volume of the object imaged [6].

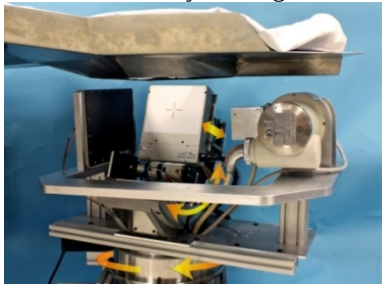

Fig. 1. Hybrid SPECT-CT breast imaging device. Orange and yellow arrows indicate the directions of movement of the SPECT camera (center).

Manuscript received November 13, 2009. This work has been funded by the National Cancer Institute of the National Institutes of Health (R01-CA096821) and the Department of Defense Breast Cancer Research Program (W81XWH-08-1-0192, W81XWH-06-1-0765 and W81XWH-06-1-0791).

KLP and MPT are with the Medical Physics Program and Radiology Department, Duke University, Durham, NC 27710 USA (telephone: 919-684-7943, e-mail: kristy.perez@duke.edu).

SJC, PM and MPT are with Biomedical Engineering and Radiology Departments, Duke University, Durham, NC 27710 USA.

B. Model System in Reconstruction Code

A flow chart outlining the steps for quantifying data with this system appears in Figure 2. Image reconstruction was performed using a ray-driven, iterative ordered-subsets expectation maximization (OSEM) reconstruction code [3]. Collimator, geometry and detection efficiencies of the SPECT camera, radiopharmaceutical half-life, and attenuation and scatter correction maps were included in the reconstruction algorithm.

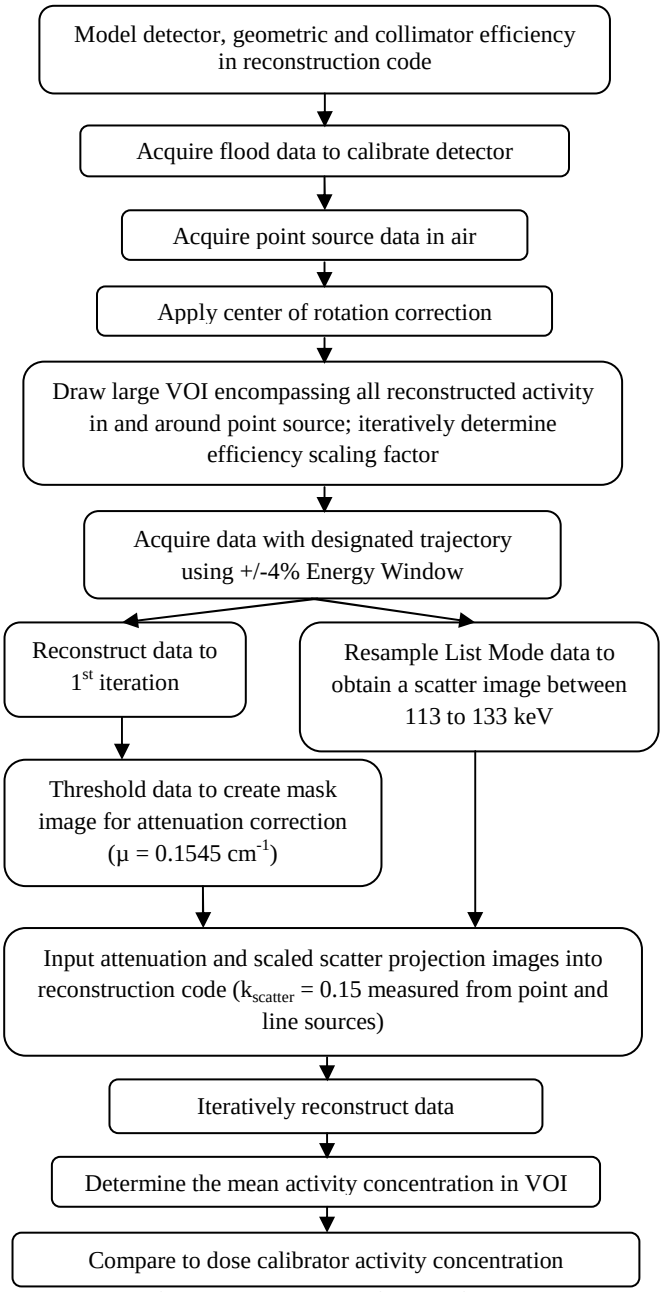

Fig 2. Flowchart of the steps to correct data for quantification.

To find the reconstruction scaling coefficient, two 0.7 mL balloons (*Harvard Apparatus*, Holliston, MA) filled with 125.5 and 115.5 μCi of ^{99m}Tc pertechnetate in 0.5 and 0.4 mL were suspended at and off the center of rotation, respectively, in a 12.5 cm diameter cylinder and were imaged with a simple circular, vertical axis of rotation (VAOR) acquisition trajectory in air. All reconstructed slices containing the point sources were summed and a region of interest was drawn encompassing all counts in the image. Equation 1 is used to determine the total activity in the reconstructed image which is compared to the dose calibrator measured activity.

$$A_{tot} = \sum_i \left[\left(A/V \right)_i V_i \right] \quad (1)$$

Where A_{tot} is the total activity in the cumulative volume of interest, i is the voxel number, A/V is the reconstructed voxel value and V is the reconstructed voxel volume. The reconstruction scaling coefficient was determined by the ratio of the measured activity concentration in the image to dose calibrator activity.

To determine the iteration at which the measured activity concentrations in the reconstructions vary the least, the data set of syringes in air was reconstructed with 8 subsets up to 100 iterations. The mean value (units of microcuries per milliliter) in a region of interest (ROI) in the reconstructed image was determined every 5 iterations for up to 100 iterations to determine the iteration where convergence is reached.

C. Geometric & Anthropomorphic Phantoms

1) Linearity Test

Three 30 mL syringes were filled with ~10 mL of clinical concentrations of aqueous ^{99m}Tc pertechnetate. The syringes were placed in a 12.5 cm diameter cylinder (Fig. 3) and imaged in air, and then in water, and water plus background activity. The initial radioactive concentrations, measured with a calibrated dose calibrator (CRC-30BC, *Capintec, Inc*., Ramsey, NJ), are given in Table I.

TABLE I: INITIAL RADIOACTIVITY AND ACTIVITY CONCENTRATION IN SYRINGES AND CYLINDER.

	Activity (uCi)	**Volume (mL)**	**Activity Conc (uCi/mL)**
Syringe 1	34.7	9.7	3.6
Syringe 2	113.3	10	11.3
Syringe 3	226.8	11	20.6
Background	386.8	900	0.430

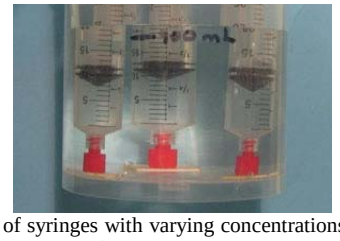

Fig. 3. Photograph of syringes with varying concentrations of radioactivity in a cylinder with an aqueous uniform radioactive background.

2) Breast & Lesion Phantoms

An 800 mL anthropomorphic breast phantom containing a 2.3 mL acrylic-walled sphere (*Radiological Service Devices Inc.*, Newport Beach, CA) and a 1.6 mL thin-walled balloon (*Harvard Apparatus*, Holliston, MA) were filled with aqueous ^{99m}Tc pertechnetate (Fig. 4). Table II gives the initial

radioactive concentrations, measured with a dose calibrator, of the spheres and background.

TABLE II: INITIAL RADIOACTIVITY AND ACTIVITY CONCENTRATION OF THE SPHERES AND BREAST PHANTOMS.

	Activity (uCi)	Volume (mL)	Activity Conc (uCi/mL)
Acrylic	28.4	2.3	12.3
Balloon	19.8	1.6	12.4
Background	222.6	765	0.291

Fig. 4. Photograph of the acrylic (left) and balloon (right) spheres in the anthropomorphic breast phantom filled with 765 mL of water.

D. *Data Acquisition*

For this data, 128 projection images collected over 360º with vertical axis of rotation (VAOR), 30º tilted parallel beam (TPB) and projected sinusoidal (PROJSINE) ranging from 15º to 45º polar tilt, paths (Fig. 5) were compared for quantification accuracy. The data was collected with a ±4% photopeak energy window centered about 140 keV.

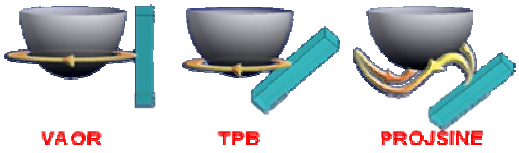

Fig. 5. 3D trajectories (yellow path) of the gamma camera (blue box) used to acquire data.

E. *Attenuation and Scatter Corrections*

We assumed a uniform emission volume to correct for signal loss due to photon attenuation. A map of the attenuation coefficients was defined by reconstructing the data to the first iteration, thresholding the image to obtain the mask of the object, and assigning each pixel a constant attenuation coefficient for water, 0.1545 cm^{-1} [7]. The original data is then reconstructed a second time implementing the uniform attenuation map along with the following scatter corrections in the reconstruction algorithm.

For scatter correction, the Compton Window Method estimates the percentage of scatter in the photopeak with a lower energy scatter window scaled by a proportionality constant, k [2]. Because a ± 4% symmetric photopeak window ranging from 134 to 146 keV was used, we chose to center the scatter window around an energy that produced a window abutting the photopeak window: 123 keV +/- 8%, ranging from 113 to 133 keV. Following the methods outlined in [2], we iteratively empirically determined k to be 0.15, consistent with previous measures in our lab.

F. *Reconstruction*

The original data was reconstructed a second time implementing the attenuation and scatter correction maps. For qualitative visual purposes and quantitative observer studies, previous studies have shown that with eight subsets the 2nd iteration gives the best SNR and contrast values [8]. To determine the optimal iteration point for quantification purposes, the image set of the syringes in air was reconstructed with eight subsets up to 100 iterations with the OSEM reconstruction code [3]. A reconstruction grid size of 150x150x150 was used. The isotropic voxel size was selected to be the same as the detector pixel size, with 2.5 mm on each side. Thus, gray scale values of the reconstructed images are output in absolute µCi/mL units.

G. *Data Analysis*

Three sagittal slices of the final converged reconstructed images were summed and ROIs were drawn in the syringe/lesions and backgrounds. ROIs for the syringes were completely within and not close to the edges of the syringes to avoid partial volume edge effects. The mean, decay corrected, reconstructed image activity concentration was determined and compared with the dose calibrator measured activity concentration. The percent difference was calculated to determine the accuracy of the reconstruction process.

III. RESULTS & DISSCUSSION

A. *Convergence of Activity Concentration Value*

The plot in Figure 6 shows that for 8 subsets, the 20th iteration will provide information that is near convergence for each trajectory.

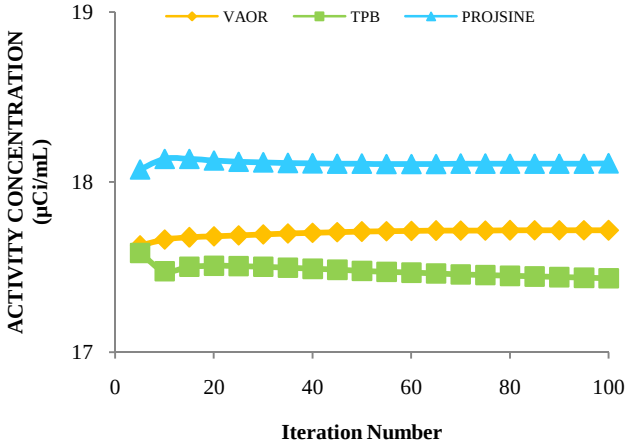

Fig. 6. Plot of mean activity concentration in an ROI as a function of iteration number. Iteration 20 was determined to be a good compromise for convergence for each of the trajectories.

B. *Linearity*

The reconstructed data shows evident differences in contrast between the variety of activity concentrations (Fig. 7). The decay corrected, mean activity concentration has good agreement with “known” values (Fig. 8). The “known” values are determined from dose calibrator measurements, which are considered as the gold standard. The results indicate that the accuracy has some dependence on both activity concentration

and acquisition trajectory. For lower activity concentrations, the accuracy is worse than for greater amounts of activity (Table III). Generally, the accuracy is better than 15% for activity concentrations >3uCi/mL. For the data with water plus radioactive background, the variability between scans is generally less than 10% for all three acquisition trajectories.

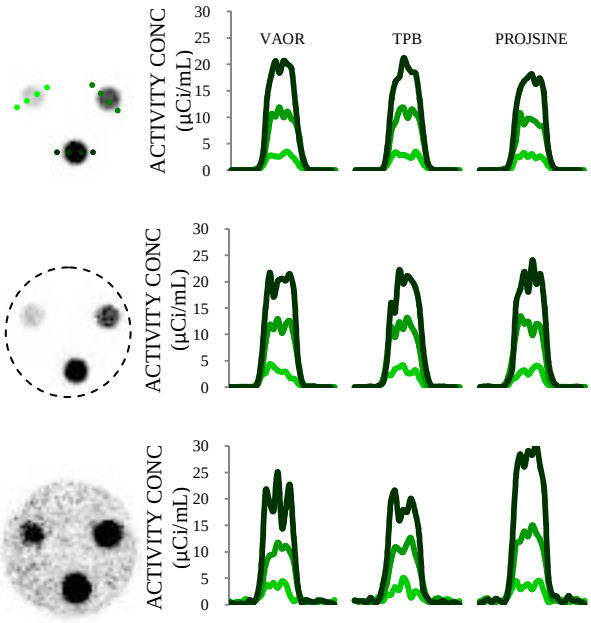

Fig. 7. Average of seven summed reconstructed slices of syringes in air (TOP, LEFT), water (MIDDLE, LEFT) and aqueous radioactivity background (BOTTOM, LEFT) acquired with a VAOR trajectory; images from other trajectories look similar. Three pixel line profiles (RIGHT) through each syringe for each acquisition.

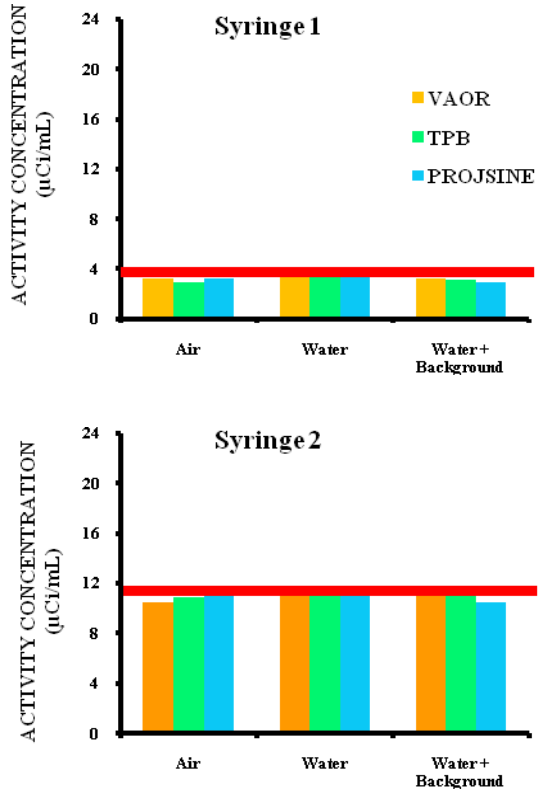

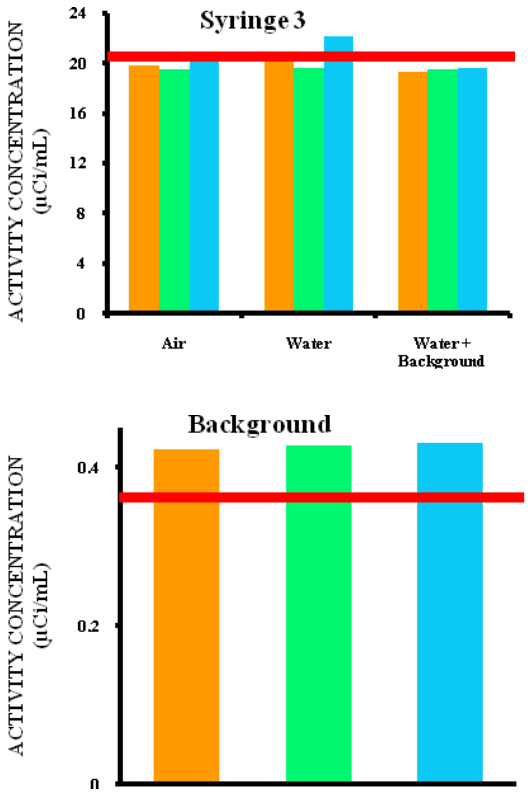

Fig. 8. Bar charts of dose calibrator (red lines) and decay corrected image measured activity concentrations for syringes 1, 2, and 3, and background.

TABLE III: PERCENT DIFFERENCE OF SYRINGES IN AIR FOR EACH ACQUISITION TRAJECTORY.

	% Difference		
	Syringe 1	**Syringe 2**	**Syringe 3**
VAOR	9.14	7.38	3.7
TPB	17.2	4.22	5.45
PROJSINE	8.84	3.36	0.4

C. Breast & Lesion

VAOR and PROJSINE spherical lesion data are accurate to within 15%, while TPB data have consistently greater than 30% deviation from the actual dose calibrator measured concentration (Fig. 10). Because the TPB data is insufficiently sampled, elongation artifacts in the reconstructed images distort the shape of the breast and lesions, dispersing the activity into a greater image volume. Additionally, there is an attenuation map inconsistency given the elongation artifact and the known, smoothly varying, true phantom distribution. Therefore, the total activity is dipersed over the larger volume, and consequently the activity concentration reported in each voxel decreases, as evident in the images set to the same global maximum in Figure 9.

The accuracy of measuring the background concentration varies greatly (Fig. 10), due to the relatively poor counting statistics of the low activity area.

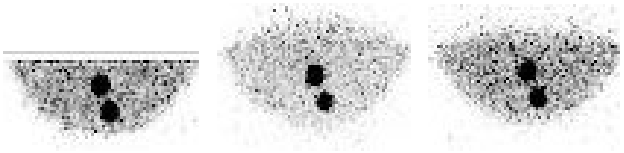

Fig. 9. MIP images of reconstructed data set to a global maximum containing acrylic (top) and thin-walled (bottom) radioactive lesion phantoms.

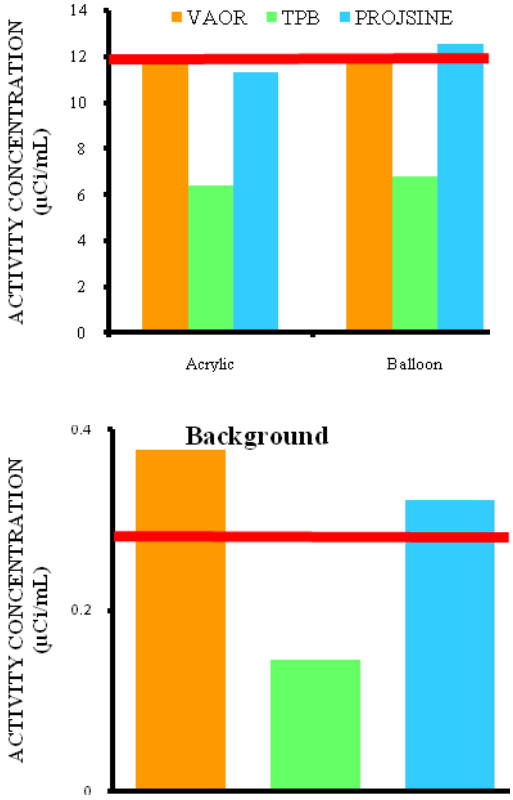

Fig. 10. Bar charts of dose calibrator (red lines) and decay corrected image measured activity concentration for the acrylic and balloon lesions (TOP) and uniform breast background (BOTTOM).

IV. Conclusions

A method to quantify the activity concentration of regions of interest in data acquired with our unique dedicated SPECT system has been implemented. The average activity concentration reported in hot-volume regions corresponds to within 15% of the actual measured activity concentrations. Larger errors persist in diffuse background regions, most likely due to the much higher noise characteristics (variability) in the background.

For this anthropomorphic breast data set, VAOR and PROJSINE data have better than 15% accuracy with respect to the absolute activity concentration. Insufficiently sampled TPB data, not unexpectedly, has the worst accuracy.

Very low activity concentrations are more difficult to accurately quantify, most likely due to their poorer counting statistics. For this study, a ±4% photopeak energy window was used, despite that part of the photopeak is cutoff due to low energy tailing using the compound semi-conductor detector system. The accuracy of quantifying low activity concentration regions by utilizing more of the photopeak events (increasing the counting statistics) will be investigated.

Additional future steps to improve results would include using the CT reconstructed data set to calculate the spatial distribution map of attenuation coefficients as well as to define the ROI for better placement, and correcting for partial volume effects. To analyze the mean activity concentration in the syringes we were able to use relatively large ROIs and place them well within the boundaries of the syringe, minimizing partial volume effects. However, for smaller and/or irregularly shaped hot spots (lesions), ROI placement has a large effect on the measured mean activity concentration. Thus, having a CT selected ROI would give more confidence in the measurement.

V. Acknowledgements

MPT is an inventor of this dedicated SPECT imaging technology, and is named as an inventor on the patent for this technology assigned to Duke. If this technology becomes commercially successful, MPT and Duke could benefit financially.

References

[1] M. S. Rosenthal, J. Cullom, W. Hawkins, S. C. Moore, B. M . Tsui and M. Yester. "Quantitative SPECT imaging: a review and recommendations by the Focus Committee of the Society of Nuclear Medicine Computer and Instrumentation Council," *J Nucl Med*, vol. 36, p. 1489-513, 1995.

[2] R. J. Jaszczak, K. L. Greer, C. E. Floyd, C. C. Harris and R. E. Coleman, "Improved SPECT Quantification Using Compensation for Scattered Photons," *J Nucl Med*, vol. 25, p. 893-900, 1984.

[3] J. E. Bowsher, V. E. Johnson, T. G. Turkington, R. J. Jaszczak, C. R. Floyd and R. E. Coleman, "Bayesian reconstruction and use of anatomical a priori information for emission tomography," *IEEE Trans on Med Img*, vol. 15 p. 673-86, 1996.

[4] C. B. Hruska and M. K. O'Conner, "Quantification of Lesion Size, Depth and Uptake Using a Dual-Head Molecular Breast Imaging System," *Med Phys*, vol. 35 p. 1365-1376, 2008.

[5] M. B. Williams, M. J. More, D. Narayanan, S. Majewski, B. Welch, R. Wojcik, and D. A. Kieper, "Phantom Study of Radiotracer Concentration Quantification in Breast Scintigraphy," *IEEE Trans Nucl Sci*, vol. 50, p. 433-438 2003.

[6] C. Archer, M. Tornai, and J. E. Bowsher, "Implementation and Initial Characterization of Acquisition Orbits with a Dedicated Emission Mammotomograph," *IEEE Trans Nucl Sci*, vol. NS50, p. 8, 2003.

[7] J. H. Hubbell and S. M. Seltzer, " http://physics.nist.gov /PhysRefData/XrayMassCoef/cover.html" *NIST*, 1996.

[8] C. N. Brzymialkiewicz, "Development and evaluation of a dedicated emission mammotomography system," Duke University, 2005.